

# Swarmalators: Oscillators that sync and swarm

Kevin P. O’Keeffe<sup>1</sup> and Steven H. Strogatz<sup>1</sup>

<sup>1</sup>*Center for Applied Mathematics, Cornell University, Ithaca, NY 14853, USA*

(ΩDated: May 2, 2022)

Synchronization occurs in many natural and technological systems, from cardiac pacemaker cells to coupled lasers. In the synchronized state, the individual cells or lasers coordinate the timing of their oscillations, but they do not move through space. A complementary form of self-organization occurs among swarming insects, flocking birds, or schooling fish; now the individuals move through space, but without conspicuously altering their internal states. Here we explore systems in which both synchronization and swarming occur together. Specifically, we consider oscillators whose phase dynamics and spatial dynamics are coupled. We call them *swarmalators*, to highlight their dual character. A case study of a generalized Kuramoto model predicts five collective states as possible long-term modes of organization. These states may be observable in groups of sperm, Japanese tree frogs, colloidal suspensions of magnetic particles, and other biological and physical systems in which self-assembly and synchronization interact.

PACS numbers: ?

## INTRODUCTION

This year marks the fiftieth anniversary of a breakthrough in the study of synchronization. In 1967, Winfree proposed a coupled oscillator model for the circadian rhythms that underlie daily cycles of activity in virtually all plants and animals [1, 2]. He discovered that above a critical coupling strength, synchronization breaks out spontaneously, in a manner reminiscent of a phase transition. Then Kuramoto simplified Winfree’s model and solved it exactly [3, 4], leading to an explosion of interest in the dynamics of coupled oscillators [5–11]. Kuramoto’s model in turn has been generalized to other large systems of biological oscillators, such as chorusing frogs [12–15], firing neurons [16–22], and even human concert audiences clapping in unison [23]. The analyses often borrow techniques from statistical physics, such as mean-field approximations, renormalization group analyses [24, 25], and finite-size scaling [26, 27]. There has also been traffic in the other direction, from biology back to physics. For example, insights from biological synchronization have shed light on neutrino oscillations [28], phase locking in Josephson junction arrays [29, 30], the dynamics of power grids [31, 32], and the unexpected wobbling of London’s Millennium Bridge on opening day [33].

A similarly fruitful interplay between physics and biology has occurred in the study of the coordinated movement of groups of animals. Fish schools, bird flocks, and insect swarms [34–40] have been illuminated by maximum entropy methods [41], agent-based simulations [42], and analytically tractable models based on self-propelled particles [43], and continuum limits [44–48].

Studies of swarming and synchronization have much in common. Both involve large, self-organizing groups of individuals interacting according to simple rules. Both lie at the intersection of nonlinear dynamics and statistical physics. Nevertheless the two fields have, by and

large, remained disconnected. Studies of swarms focus on how animals move, while neglecting the dynamics of their internal states. Studies of synchronization do the opposite: they focus on oscillators’ internal dynamics, not on their motion. In the past decade, however, a few studies of “mobile oscillators,” motivated by applications in robotics and developmental biology, have brought the two fields into contact [49–53]. Even so, the assumption has been that the oscillators’ locations affect their phase dynamics, but not conversely. Their motion has been modeled as a random walk or as externally determined, without feedback from the oscillators’ phases.

We suspect that somewhere in nature and technology there must be mobile oscillators whose phases affect how they move. For instance, many species of frogs, crickets, and katydids call periodically, and synchronize in vast choruses [54–56]. When the individuals hop around, do they tend to move toward or away from others, depending on the relative phases of their calling rhythms? If so, what spatiotemporal patterns would we expect?

A clue comes from the physics of magnetic colloids [57–59] and microfluidic mixtures of active spinners [60, 61], both of which show rich collective behavior. In these systems, the particles or spinners attract or repel one another, depending on their orientations. Given that orientation is formally analogous to the phase of an oscillation (both being circular variables), a similarly rich phenomenology is expected for mobile oscillators whose phases affect their motion. We call these hypothetical systems *swarmalators* because they generalize swarms and oscillators.

Here we analyze one of the simplest models of a swarmalator system. Its simplicity allows some of its collective states and bifurcations to be derived analytically. We hope that the resulting predictions will stimulate the discovery and characterization of natural and technological systems of swarmalators.

## THE MODEL

We consider swarmalators free to move in the plane. The governing equations are

$$\dot{\vec{x}}_i = \frac{1}{N} \sum_{j=1}^N \vec{I}_{att}(\vec{x}_j - \vec{x}_i) F(\theta_j - \theta_i) - \vec{I}_{rep}(\vec{x}_j - \vec{x}_i), \quad (1)$$

$$\dot{\theta}_i = \omega_i + \frac{K}{N} \sum_{j=1}^N G_{att}(\theta_j - \theta_i) H(\vec{x}_j - \vec{x}_i), \quad (2)$$

for  $i = 1, \dots, N$ , where  $\vec{x}_i, \theta_i, \omega_i$  are the position, phase, and natural frequency of the  $i$ -th swarmalator, and  $N$  is the population size. The functions  $\vec{I}_{att}, \vec{I}_{rep}$  represent the spatial attraction and repulsion between swarmalators, while the phase interaction is captured by  $G_{att}$ . The function  $F$  measures the influence of phase similarity on spatial attraction, while  $H$  measures the influence of spatial proximity on the phase dynamics.

Consider the following instance of this model:

$$\dot{\vec{x}}_i = \frac{1}{N} \sum_{j,j \neq i}^N \frac{\vec{x}_j - \vec{x}_i}{|\vec{x}_j - \vec{x}_i|} \left( A + J \cos(\theta_j - \theta_i) \right) - B \frac{\vec{x}_j - \vec{x}_i}{|\vec{x}_j - \vec{x}_i|^2} \quad (3)$$

$$\dot{\theta}_i = \omega_i + \frac{K}{N} \sum_{j,j \neq i}^N \frac{\sin(\theta_j - \theta_i)}{|\vec{x}_j - \vec{x}_i|}. \quad (4)$$

We choose power laws for  $I_{att}, I_{rep}$  and  $H$  for simplicity. The exponents of these power laws were chosen to make our analysis as simple as possible (as we show in a stability analysis in [62]). We also choose the sine function for  $G_{att}$  for simplicity, in the spirit of the Kuramoto model [3, 4]. By rescaling time and space, we set the parameters  $A, B$  to 1, and by going to a suitable frame, we set  $\omega_i = 0$ , all without a loss of generality. This leaves us with a system with two parameters  $(J, K)$ .

The parameter  $K$  is the phase coupling strength. For  $K > 0$ , the phase coupling between swarmalators tends to minimize their phase difference, while for  $K < 0$ , this phase difference is maximized. The parameter  $J$  measures the extent to which phase similarity enhances spatial attraction. For  $J > 0$ , “like attracts like”: swarmalators prefer to be near other swarmalators with the same phase. When  $J < 0$ , we have the opposite scenario: swarmalators are preferentially attracted in space to those with *opposite* phase. And when  $J = 0$ , swarmalators are phase-agnostic, their spatial attraction being independent of their phase. To keep  $I_{att}(x) > 0$ , we constrain  $J$  to satisfy  $-1 \leq J \leq 1$ .

## RESULTS

To probe the behavior of our system, we performed numerical experiments using python’s ODE solver ‘odeint’. We initially positioned the swarmalators in a box of length 2, and drew their phases from  $[\pi, \pi]$ , both uniformly at random. We found the system settles into five states. In three of these states, the swarmalators are ultimately stationary in space and phase. In the remaining two, the swarmalators are non-stationary. However in all states, the density of swarmalators  $\rho(\vec{x}, \theta, t)$  is time-independent, where  $\rho(\vec{x}, \theta, t) d\vec{x} d\theta$  gives the fraction of swarmalators with positions between  $\vec{x}$  and  $\vec{x} + d\vec{x}$ , and phases between  $\theta$  and  $\theta + d\theta$  at time  $t$ . In Figure 1 we show where these states occur in the  $(J, K)$  parameter plane. We next discuss these states.

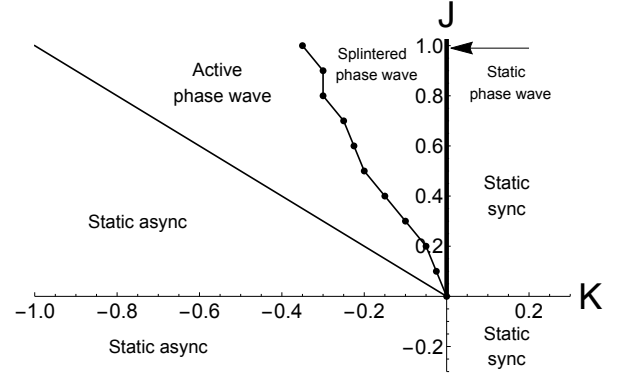


FIG. 1: Phase diagram for the model defined by (3), (4). The straight line separating the static async and active phase wave states was calculated analytically and is given by Eq. (11). The dotted line separating the active phase wave and splintered phase wave states was calculated numerically, where black dots show simulation results.

**Static synchrony.** The first state is shown in Figure 2(a). The swarmalators form a circularly symmetric, crystal-like distribution in space, and are fully synchronized in phase, as indicated by all of them having the same color in Figure 2(a). Since the swarmalators are ultimately stationary in  $\vec{x}$ , and they all end up at the same phase  $\theta$ , we call this the *static sync* state. It occurs for  $K > 0$  and for all  $J$ , as seen in Figure 1.

In the continuum limit, this state is described by  $\rho(r, \phi, \theta, t) = \frac{1}{2\pi} g(r) \delta(\theta - \theta_0)$ , where  $\phi$  is the spatial angle  $\phi = \arctan(y/x)$ , and the final phase  $\theta_0$  is determined from the initial conditions. In [62] we use the continuity equation for  $\rho(\vec{x}, \theta, t)$  to derive a set of self-consistency equations for  $g(r)$ , which we were unable to solve. However, if a linear attraction kernel,  $\vec{I}_{att}(\vec{x}) = \vec{x}$ , is used instead of the unit vector kernel  $\vec{I}_{att}(\vec{x}) = \vec{x}/|\vec{x}|$  we are currently considering, then the solution is  $g(r) = 1$ , i.e., the swarmalators are uniformly distributed in a disc of radius  $R$ . In this special case, we can also calculate  $R$  analytically:

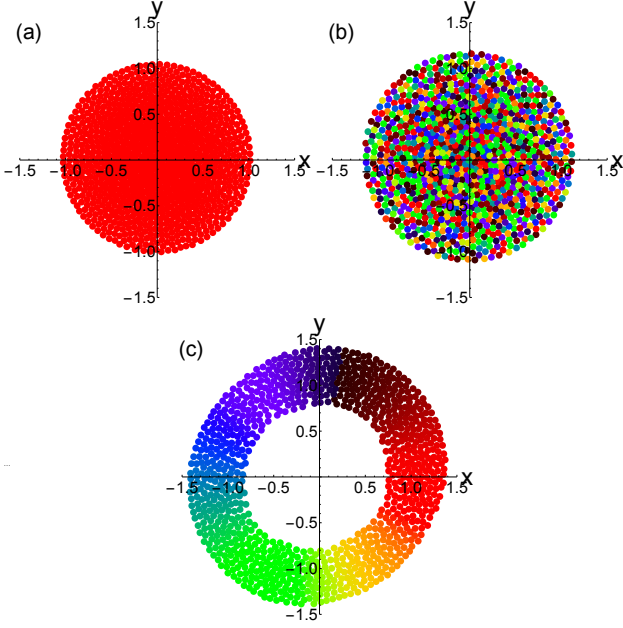


FIG. 2: Scatter plots of three states in the  $(x, y)$  plane, where the swarmalators are colored according to their phase. In each plot,  $N = 1000$  swarmalators for 100 time units with a step of  $dt = 0.1$ . (a) Static sync state for  $(J, K) = (0.1, 1)$ . (b) Static async state  $(J, K) = (0.1, -1)$ . (c) Static phase wave state  $(J, K) = (1, -0.25)$

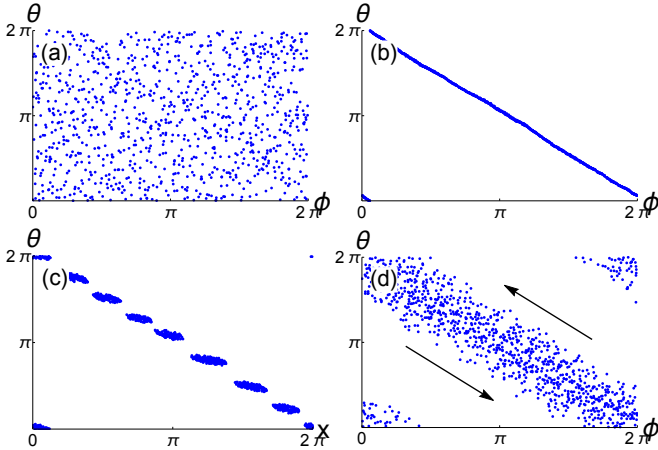


FIG. 3: Distributions of different states in  $(\phi, \theta)$  space, where  $\phi = \arctan(y/x)$ . In panels, simulations were run with  $N = 1000$  swarmalators for 500 time units with a step of  $dt = 0.1$ . (a) Static async state for  $(J, K) = (0.1, -1)$ . (b) Static phase wave state  $(J, K) = (1, 0)$  (c) Splintered phase wave state  $(J, K) = (1, -0.25)$ . (d) Active phase wave state  $(J, K) = (1.0, -0.75)$ . Black arrows indicate the shear flow motion of swarmalators

$$R_{sync} = \sqrt{\frac{1}{1+J}}. \quad (5)$$

In dimensionful units, this reads  $R = \sqrt{B/(A+J)}$ .

Thus the radius is determined by the ratio of the strengths of the attractive to the repulsive forces  $I_{att}, I_{rep}$  (in the static sync state, the effective attraction force is  $A+J \cos(\theta_j - \theta_i) = A+J$ , since all swarmalators have the same phase). Figure 4(a) shows the prediction (5) against simulation results. Good agreement is evident.

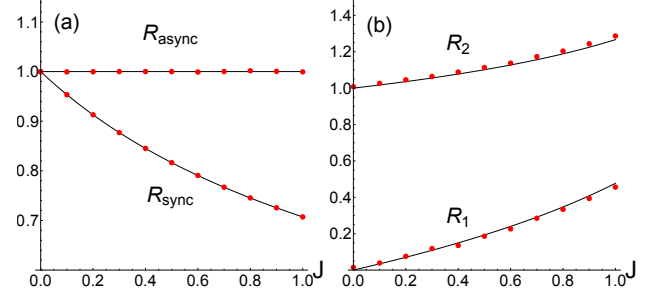


FIG. 4: Radii of stationary states for  $N = 800$  swarmalators for a linear attraction kernel  $I_{att}(\vec{x}) = \vec{x}$ . Red dots show simulation data, while black curves show theoretical predictions. (a): Radius of crystal formed in static sync state (for  $K = 1$ ) and static async state (for  $K = -2$ ) versus  $J$ . (b): Inner and outer radii of annulus in static phase wave state versus  $J$ .

**Static asynchrony.** Swarmalators can also form a *static async* state, illustrated in Figure 2(b). At any given location  $\vec{x}$ , all phases  $\theta$  can occur, and hence all colors are present everywhere in Figure 2(b). This is seen more clearly in a scatter plot of the swarmalators in the  $(\phi, \theta)$  plane, depicted in Figure 3(a). Notice that the swarmalators are distributed uniformly, meaning that every phase occurs everywhere. This completely asynchronous state occurs in the quadrant  $J < 0, K < 0$ , and also for  $J > 0$  as long as  $J$  lies in the wedge  $J < |K_c|$  shown in the phase diagram in Figure 1. As for the static sync state, we were able to calculate the radius of the circular distribution when a linear attraction kernel  $\vec{I}(\vec{x})$  was used. In [62] we show this radius is given by

$$R_{async} = 1 \quad (6)$$

which agrees with simulation as shown in Figure 4(a).

**Static phase-wave.** The final stationary state occurs for the special case  $K = 0$  and  $J > 0$ . This means the swarmalators' phases are frozen at their initial values. How, then, does the population evolve? Since  $J > 0$ , 'like attracts like': swarmalators want to settle near others with similar phase. The result is an annular structure where the spatial angle  $\phi$  of each swarmalator is perfectly correlated with its phase  $\theta$ , as seen in Figures 2(c) and 3(b). Since the phases run through a full cycle as the swarmalators arrange themselves around the ring, we call this state the *static phase wave*.

In density space, this static phase wave state is described by  $\rho(r, \phi, \theta) = g(r)\delta(\phi \pm \theta + C_1)$  where the  $\pm$  and

the constant  $C_1$ , are determined by the initial conditions. In [62] we again consider the linear attraction kernel, and find that  $g(r)$  can be obtained analytically as

$$g(r) = 1 - \frac{\Gamma_J}{r}, \quad R_1 \leq r \leq R_2 \quad (7)$$

with  $\Gamma_J = 2J(R_2^3 - R_1^3)(3J(R_2^2 - R_1^2) + 12)^{-1}$ . This in turns lets us calculate the inner and outer radii  $R_1, R_2$  of the annulus:

$$R_1 = \Delta_J \frac{12\sqrt{3} - \sqrt{3}J + 3\sqrt{12 - 5J}\sqrt{4 + J}}{12J}, \quad (8)$$

$$R_2 = \frac{\Delta_J}{2\sqrt{3}}, \quad (9)$$

with  $\Delta_J = \sqrt{(-12 + 3J + \sqrt{36 - 15J}\sqrt{4 + J})/(J - 2)}$ . Figure 4(b) shows agreement between these predictions and simulation.

**Splintered phase wave.** Moving from  $K = 0$  into the  $K < 0$  plane, we encounter the first non-stationary state, shown in Figure 5(a) and Figure 3(c). As can be seen, the static phase-wave divides into disconnected clusters of distinct phases. Accordingly we call this state the *splintered phase wave*. The number of clusters is controlled by the length scale of the interaction functions  $\bar{I}_{att}(\vec{x}), \bar{I}_{rep}(\vec{x}), H(\vec{x})$ : smaller length scales lead to more clusters. Within each cluster, the swarmalators “quiver,” executing small amplitude oscillations in both position and phase about their mean values.

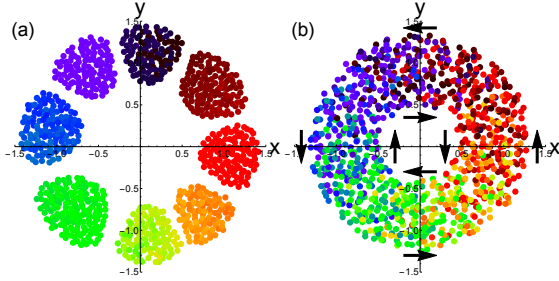


FIG. 5: Two non-steady states for  $N = 1000$  swarmalators with a time step of 0.1. In all cases, swarmalators were initially placed in a box of length 2 uniformly at random, while their phases were drawn from  $[-\pi, \pi]$ . (a) Splintered phase wave  $(J, K) = (1, -0.25)$ . (b) Active phase wave  $(J, K) = (1, -0.75)$ .

**Active phase wave.** As  $K$  is further decreased, these oscillations increase in amplitude until the swarmalators start to execute uniform circular motion in both position and phase. The direction of rotation depends on their radial position; there is shear flow. Swarmalators

closer to the inner radius rotate in one direction, while those closer to the outer radius rotate in the opposite direction, as indicated schematically by the black arrows in Figures 5(b) and 3(d). A similar kind of shear flow is seen in the double milling states found in models of biological swarming [63].

At the density level, this new, and final, state is like a blurred version of the static phase wave, insofar as the spatial angle and phase of a given swarmalator are roughly correlated, as evident in Figure 3(d). However unlike the static phase wave, the swarmalators are non-stationary. To highlight this difference, we name this state the *active phase wave*.

**Order parameters.** Having described the five states of our system, we next discuss how to distinguish them. We define the following order parameter,

$$W_{\pm} = S_{\pm} e^{i\Psi_{\pm}} = \frac{1}{N} \sum_{j=1}^N e^{i(\phi_j \pm \theta_j)}, \quad (10)$$

where  $\phi_i := \arctan(y_i/x_i)$ . As shown in Figure 6, the magnitude  $S_{\pm}$  varies from 1 to 0 as we decrease  $K$  from 0, passing through all the states in the upper left quadrant of the  $(J, K)$  plane. (Note that all states except for static sync occur in this part of parameter space, so we hereafter confine our attention to this region.)

To see why  $S_{\pm}$  varies in this manner, recall that in the static phase wave state, the spatial angle and phase of each swarmalator are perfectly correlated,  $\phi_i = \pm\theta_i + C_1$  (recall that the  $\pm$  and  $C_1$  are determined by the initial conditions). Therefore  $S_{\pm} = 1$  at  $K = 0$ , where the static phase wave state is realized. Decreasing  $K$ , the correlation between  $\phi_i$  and  $\theta_i$  gets weaker and weaker as we pass through the splintered, and active, phase wave states. This loss of correlation progressively diminishes  $S_{\pm}$ , until it finally drops to zero when the static async state is reached, in which  $\phi_i$  and  $\theta_i$  are fully uncorrelated.

To sum up,  $S_{\pm}$  is zero in the static async state, bifurcates from zero at a critical coupling strength  $K_c$ , is non-zero in the non-stationary splintered and active phase wave states, and is one in the static phase wave state. In [62] we calculate this critical  $K_c$  by performing a linear stability analysis in density space. The critical value is simply

$$K_c = -J, \quad (11)$$

which agrees with simulation as shown in Figure 6.

Notice however that since  $S_{\pm}$  is non-zero for both the splintered and active phase wave, it cannot distinguish between these states. To do this, we define another order parameter, denoted by  $\gamma$ . It is defined as the

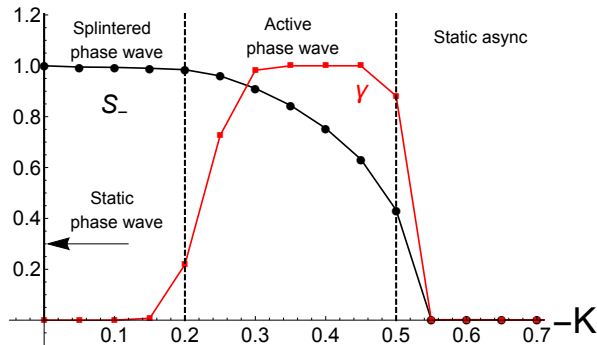


FIG. 6: Asymptotic behavior of the order parameter  $S$  (black dots) and  $\gamma$  (red dots) for  $J = 0.5$  and  $N = 500$  swarmalators. Data was collected for  $T = 500$  time units, of which the first half were discarded as transients. Note that the data are plotted versus  $-K$  rather than  $K$ . The order parameter  $S_-$  bifurcates from 0 at  $K_c = -J = -0.5$ , as per Eq. (11).

fraction of swarmalators that have executed at least one full cycle in phase and position, after transients have been discarded. Then  $\gamma$  is zero for the splintered phase wave, and non-zero for the active phase wave. Using  $\gamma$  in concert with  $S_{\pm}$  then allows us to distinguish among all the states, as illustrated in Figure 6.

**Genericity.** Our analysis so far has been for a particular instance (3), (4), of the model defined by (1), (2). This begs the question: are the phenomena we found generic to the model? Or specific to this instance of the model? To explore this issue, we ran simulations for different choices of the functions  $\vec{I}_{rep}(\vec{x})$ ,  $\vec{I}_{att}(\vec{x})$ ,  $H(\vec{x})$ . Specifically, we chose

$$\vec{I}_{rep}(x) = \frac{\vec{x}}{|\vec{x}|^4}, \quad (12)$$

$$\vec{I}_{att}(x) = \frac{\vec{x}}{|\vec{x}|^2} \text{ or } \vec{x}, \quad (13)$$

$$H(x) = \frac{1}{|\vec{x}|^2} \text{ or } \exp(-|\vec{x}|). \quad (14)$$

In all but one case, we found the same phenomena.

The exception is the linear attraction kernel  $\vec{I}_{att}(\vec{x}) = \vec{x}$  (which is not surprising, given that it is qualitatively different to the other power law decay interactions considered). Here we found new states, which we collectively call *traveling phase waves*. They are similar to the active phase wave states, except now the offset in the correlation between the spatial angle and phase of a given swarmalator becomes periodic in time:  $\phi_i \approx \theta_i + C_1(t)$ . Equivalently, the phase  $\Psi_{\pm}$  of the order parameter  $W_{\pm}$  begins to rotate, reminiscent of the traveling wave states found in the Kuramoto model with distributed coupling strengths [64, 65]. This new feature means the density  $\rho(\vec{x}, \theta, t)$ , as

well as the individual swarmalators, are non-stationary, in sharp distinction to all the other states previously encountered. We further discuss this and other properties of the traveling phase waves in [62].

## DISCUSSION

We have examined the collective dynamics of swarmalators. These are mobile particles or agents with both spatial and internal degrees of freedom, which lets them sync and swarm. Furthermore, their spatial and phase dynamics are coupled. By studying simple models, we found this coupling leads to rich spatiotemporal patterns which we explored analytically and numerically.

The most pertinent future goal is to find and investigate the behavior of real-world systems of swarmalators. As mentioned in the introduction, colloidal suspensions of magnetic particles [57–59] or active spinners [60, 61] are promising candidates. For example, structures equivalent to the static phase wave state have been experimentally realized by Snezhko and Aranson, when studying the behavior of ferromagnetic colloids at liquid-liquid interfaces [58] (the particles comprising the colloids can be considered swarmalators if we interpret the angle subtended by their magnetic dipole vectors as their phase). As illustrated in Figure 4 of [58], the colloids can form “asters.” These are structures composed of radial chains of magnetically ordered particles, which “decorate slopes of a self-induced circular standing wave” [58], analogous to the annular pattern of correlated phases and positions of the static phase wave shown in Figure 2(c).

Could colloidal equivalents of the splintered and active phase wave states also be realized? Aside from being theoretically interesting, the ability to engineer these states could have practical application. For instance, Snezhko and Aranson also show that asters can be manipulated to capture and transport target particles. Perhaps the non-stationary behavior of the splintered and active wave states could also have locomotive utility. Tentative evidence for this claim is provided by populations of cilia, whose collective metachronal waves, similar to the motion of swarmalators in the aforementioned states, are known to facilitate biological transport [66–70].

Other plausible systems of real-world swarmalators are biological microswimmers, self-propelled microorganisms capable of collective behavior [71]. One such contender is populations of spermatozoa, which exhibit rich swarming behavior such as trains [72, 73] and vortex arrays [74]. Here the phase variable is associated with the rhythmic beating of the sperm’s tail, which can synchronize with that of a neighboring sperm [75, 76]. It has been theorized that this can induce spatial attraction [77], leading to clusters of synchronized sperm, consistent with experimentally observed behavior [78, 79].

Lastly, there are also theoretical avenues to explore within our proposed model of swarmalators. For example, our model is kinematic: first order in time, meaning the velocity of each swarmalator is uniquely determined by its position and phase. Dynamic models, where the velocity has its own evolution equation, are more realistic and lead to qualitatively new behavior. Further realism could be incorporated by including heterogeneity in the natural frequencies  $\omega_i$  and the coupling parameters  $K, J$ , and by considering delayed or noisy interactions. Letting the swarmalators move in three spatial dimensions could also be interesting.

### ACKNOWLEDGMENTS

Research supported by NSF Grant Nos. DMS-1513179 and CCF-1522054.

- 
- [1] A. T. Winfree, *Journal of Theoretical Biology* **16**, 15 (1967).
  - [2] A. T. Winfree, *The Geometry of Biological Time* (Springer, 2001).
  - [3] Y. Kuramoto, in *International Symposium on Mathematical Problems in Theoretical Physics*, edited by H. Araki (Springer, 1975), pp. 420–422.
  - [4] Y. Kuramoto, *Chemical Oscillations, Waves, and Turbulence* (Springer, 1984).
  - [5] S. Strogatz, *Sync: The Emerging Science of Spontaneous Order* (Hyperion, 2003).
  - [6] A. Pikovsky, M. Rosenblum, and J. Kurths, *Synchronization: A Universal Concept in Nonlinear Sciences* (Cambridge University Press, 2003).
  - [7] S. H. Strogatz, *Physica D: Nonlinear Phenomena* **143**, 1 (2000).
  - [8] J. A. Acebrón, L. L. Bonilla, C. J. P. Vicente, F. Ritort, and R. Spigler, *Reviews of Modern Physics* **77**, 137 (2005).
  - [9] F. Dörfler and F. Bullo, *Automatica* **50**, 1539 (2014).
  - [10] A. Pikovsky and M. Rosenblum, *Chaos* **25**, 097616 (2015).
  - [11] F. A. Rodrigues, T. K. D. Peron, P. Ji, and J. Kurths, *Physics Reports* **610**, 1 (2016).
  - [12] I. Aihara, S. Horai, H. Kitahata, K. Aihara, and K. Yoshikawa, *IEICE Transactions on Fundamentals of Electronics, Communications and Computer Sciences* **90**, 2154 (2007).
  - [13] I. Aihara, H. Kitahata, K. Yoshikawa, and K. Aihara, *Artificial Life and Robotics* **12**, 29 (2008).
  - [14] I. Aihara, *Phys. Rev. E* **80**, 011918 (2009).
  - [15] I. Aihara, T. Mizumoto, T. Otsuka, H. Awano, K. Nagira, H. G. Okuno, and K. Aihara, *Scientific Reports* **4**, 3891 (2014).
  - [16] E. Montbrió, D. Pazó, and A. Roxin, *Physical Review X* **5**, 021028 (2015).
  - [17] D. Pazó and E. Montbrió, *Physical Review X* **4**, 011009 (2014).
  - [18] T. B. Luke, E. Barreto, and P. So, *Neural computation* **25**, 3207 (2013).
  - [19] T. B. Luke, E. Barreto, and P. So, *Frontiers in computational neuroscience* **8** (2014).
  - [20] K. P. O’Keefe and S. H. Strogatz, *Physical Review E* **93**, 062203 (2016).
  - [21] Y. Kuramoto, S. Shinomoto, and H. Sakaguchi, in *Mathematical Topics in Population Biology, Morphogenesis, and Neurosciences, Lecture Notes in Biomathematics, Vol. 71*, edited by E. Teramoto and M. Yamaguti (Springer, Berlin, 1987), pp. 329–337.
  - [22] C. R. Laing, *Physical Review E* **90**, 010901 (2014).
  - [23] Z. Neda, E. Ravasz, T. Vicsek, Y. Brechet, and A. L. Barabási, *Phys. Rev. E* **61**, 6987 (2000).
  - [24] H. Daido, *Physical Review Letters* **61**, 231 (1988).
  - [25] P. Östborn, *Physical Review E* **79**, 051114 (2009).
  - [26] H. Hong, H. Chaté, H. Park, and L.-H. Tang, *Physical Review Letters* **99**, 184101 (2007).
  - [27] H. Hong, H. Chaté, L.-H. Tang, and H. Park, *Physical Review E* **92**, 022122 (2015).
  - [28] J. Pantaleone, *Phys. Rev. D* **58**, 073002 (1998).
  - [29] K. Wiesenfeld, P. Colet, and S. H. Strogatz, *Physical Review Letters* **76**, 404 (1996).
  - [30] K. Wiesenfeld and J. W. Swift, *Phys. Rev. E* **51**, 1020 (1995).
  - [31] A. E. Motter, S. A. Myers, M. Anghel, and T. Nishikawa, *Nature Physics* **9**, 191 (2013).
  - [32] F. Dörfler and F. Bullo, *SIAM Journal on Control and Optimization* **50**, 1616 (2012).
  - [33] S. H. Strogatz, D. M. Abrams, A. McRobie, B. Eckhardt, and E. Ott, *Nature* **438**, 43 (2005).
  - [34] I. D. Couzin, J. Krause, R. James, G. D. Ruxton, and N. R. Franks, *Journal of Theoretical Biology* **218**, 1 (2002).
  - [35] I. D. Couzin and J. Krause, *Advances in the Study of Behavior* **32**, 1 (2003).
  - [36] I. Couzin, *Nature* **445**, 715 (2007).
  - [37] J. Buhl, D. J. Sumpter, I. D. Couzin, J. J. Hale, E. Despland, E. Miller, and S. J. Simpson, *Science* **312**, 1402 (2006).
  - [38] D. J. Sumpter, *Collective Animal Behavior* (Princeton University Press, 2010).
  - [39] J. E. Herbert-Read, *Journal of Experimental Biology* **219**, 2971 (2016).
  - [40] M. Ballerini, N. Cabibbo, R. Candelier, A. Cavagna, E. Cisbani, I. Giardina, V. Lecomte, A. Orlandi, G. Parisi, A. Procaccini, et al., *Proceedings of the National Academy of Sciences* **105**, 1232 (2008).
  - [41] W. Bialek, A. Cavagna, I. Giardina, T. Mora, E. Silvestri, M. Viale, and A. M. Walczak, *Proceedings of the National Academy of Sciences* **109**, 4786 (2012).
  - [42] C. W. Reynolds, *ACM SIGGRAPH Computer Graphics* **21**, 25 (1987).
  - [43] T. Vicsek, A. Czirók, E. Ben-Jacob, I. Cohen, and O. Shochet, *Physical Review Letters* **75**, 1226 (1995).
  - [44] A. J. Bernoff and C. M. Topaz, *SIAM Review* **55**, 709 (2013).
  - [45] C. M. Topaz and A. L. Bertozzi, *SIAM Journal on Applied Mathematics* **65**, 152 (2004).
  - [46] C. M. Topaz, A. L. Bertozzi, and M. A. Lewis, *Bulletin of Mathematical Biology* **68**, 1601 (2006).
  - [47] A. J. Leverentz, C. M. Topaz, and A. J. Bernoff, *SIAM Journal on Applied Dynamical Systems* **8**, 880 (2009).

- [48] T. Kolokolnikov, H. Sun, D. Uminsky, and A. L. Bertozzi, *Physical Review E* **84**, 015203 (2011).
- [49] K. Uriu, S. Ares, A. C. Oates, and L. G. Morelli, *Physical Review E* **87**, 032911 (2013).
- [50] I. V. Belykh, V. N. Belykh, and M. Hasler, *Physica D: Nonlinear Phenomena* **195**, 188 (2004).
- [51] D. J. Stilwell, E. M. Bollt, and D. G. Roberson, *SIAM Journal on Applied Dynamical Systems* **5**, 140 (2006).
- [52] M. Frasca, A. Buscarino, A. Rizzo, L. Fortuna, and S. Boccaletti, *Physical Review Letters* **100**, 044102 (2008).
- [53] N. Fujiwara, J. Kurths, and A. Díaz-Guilera, *Physical Review E* **83**, 025101 (2011).
- [54] T. J. Walker, *Science* **166**, 891 (1969).
- [55] E. Sismondo, *Science* **249**, 55 (1990).
- [56] M. D. Greenfield, *American Zoologist* **34**, 605 (1994).
- [57] J. Yan, M. Bloom, S. C. Bae, E. Luijten, and S. Granick, *Nature* **491**, 578 (2012).
- [58] A. Snezhko and I. S. Aranson, *Nature Materials* **10**, 698 (2011).
- [59] J. E. Martin and A. Snezhko, *Reports on Progress in Physics* **76**, 126601 (2013).
- [60] N. H. Nguyen, D. Klotz, M. Engel, and S. C. Glotzer, *Physical Review Letters* **112**, 075701 (2014).
- [61] B. C. van Zuiden, J. Paulose, W. T. Irvine, D. Bartolo, and V. Vitelli, *Proceedings of the National Academy of Sciences* **113**, 12919 (2016).
- [62] *Supplemental Materials* (2017).
- [63] J. Carrillo, M. Dorsogna, and V. Panferov, *Kinetic and Related Models* **2**, 363 (2009).
- [64] H. Hong and S. H. Strogatz, *Physical Review Letters* **106**, 054102 (2011).
- [65] H. Hong, K. P. O’Keeffe, and S. H. Strogatz, *Physical Review E* **93**, 022219 (2016).
- [66] J. Elgeti and G. Gompper, *Proceedings of the National Academy of Sciences* **110**, 4470 (2013).
- [67] S. Nonaka, Y. Tanaka, Y. Okada, S. Takeda, A. Harada, Y. Kanai, M. Kido, and N. Hirokawa, *Cell* **95**, 829 (1998).
- [68] Y. Okada, S. Nonaka, Y. Tanaka, Y. Saijoh, H. Hamada, and N. Hirokawa, *Molecular Cell* **4**, 459 (1999).
- [69] P. Satir and M. A. Sleight, *Annual Review of Physiology* **52**, 137 (1990).
- [70] L. Wong, I. F. Miller, and D. B. Yeates, *Journal of Applied Physiology* **75**, 458 (1993).
- [71] E. Lauga and T. R. Powers, *Reports on Progress in Physics* **72**, 096601 (2009).
- [72] S. Immler, H. D. Moore, W. G. Breed, and T. R. Birkhead, *PloS one* **2**, e170 (2007).
- [73] H. Moore, K. Dvůřáková, N. Jenkins, and W. Breed, *Nature* **418**, 174 (2002).
- [74] I. H. Riedel, K. Kruse, and J. Howard, *Science* **309**, 300 (2005).
- [75] G. Taylor, *Proceedings of the Royal Society of London A: Mathematical, Physical and Engineering Sciences* **209**, 447 (1951).
- [76] L. J. Fauci and A. McDonald, *Bulletin of Mathematical Biology* **57**, 679 (1995).
- [77] Y. Yang, J. Elgeti, and G. Gompper, *Physical Review E* **78**, 061903 (2008).
- [78] F. Hayashi, *Functional Ecology* **12**, 347 (1998).
- [79] F. Hayashi, *Journal of Insect Physiology* **42**, 859 (1996).